Mean Atlantic meridional overturning circulation across 26.5°N from eddy-resolving simulations compared to observations

X. Xu,[1] W. J. Schmitz Jr.,[2] H. E. Hurlburt,[3] and P. J. Hogan[3]

Received 7 September 2011; revised 10 February 2012; accepted 13 February 2012; published 30 March 2012.

[1] Observations along 26.5°N are used to examine the time mean structure of the Atlantic meridional overturning circulation (AMOC) in eddy-resolving simulations with the Hybrid Coordinate Ocean Model (HYCOM). The model results yield a 5 year mean AMOC transport of 18.2 Sv, compared to 18.4 Sv based on data. The modeled northward limb of the AMOC has a vertical structure similar to observations. The southward limb is shallower than observed but deeper than other ocean general circulation models and includes a secondary transport maximum near 4000 m corresponding to Nordic Seas Overflow Water. The modeled flow through the Florida Strait and the deep western boundary current (DWBC) east of Abaco, Bahamas, are also approximately consistent with observations. The model results are used to clarify the sources of the northward AMOC transport and to explore the circulation pattern of the southward transport in the western subtropical North Atlantic in the range 18–33°N. About 14.1 Sv of the modeled northward AMOC transport is through the Florida Strait and the remainder through the mid-ocean, primarily in the Ekman layer, but also below 600 m. The modeled AMOC transport is about 2/3 surface water and 1/3 Antarctic Intermediate Water with no contribution from the thermocline water in between. In the western subtropical North Atlantic the model results depict a complicated deep circulation pattern, associated with the complex bathymetry. The DWBC flows southward then eastward in both the upper and lower North Atlantic Deep Water (NADW) layers but with different offshore recirculation pathways, and there exists a second, more northern branch of eastward flow in the lower NADW layer.

Citation: Xu, X., W. J. Schmitz Jr., H. E. Hurlburt, and P. J. Hogan (2012), Mean Atlantic meridional overturning circulation across 26.5°N from eddy-resolving simulations compared to observations, *J. Geophys. Res.*, *117*, C03042, doi:10.1029/2011JC007586.

1. Introduction

[2] The Atlantic meridional overturning circulation (AMOC hereafter) consists of a net northward flow of warm water in approximately the upper 1000 m that overlays a net southward flow of cold water. It carries a northward oceanic heat flux greater than 1 PW in the subtropical North Atlantic [*Hall and Bryden*, 1982], or about 1/4 of the total heat transported via the global ocean-atmosphere system [*Wunsch*, 2005]. Recognizing its importance to the Earth's climate system, the joint U.K.-U.S. Rapid Climate Change-MOC program has monitored the trans-basin AMOC continuously since March 2004 using a moored instrument array deployed along 26.5°N in the Atlantic [*Cunningham et al.*, 2007; *Kanzow et al.*, 2007]. The transport and structure of the western boundary current components of the AMOC, including the Florida Current (FC) through the Strait of Florida and the deep western boundary current (DWBC) to the east of Abaco, Bahamas, have also been relatively well-established. These observations provide a unique benchmark for evaluating ocean general circulation model (OGCM) performance in simulating this important circulation feature.

[3] Some aspects of the time mean AMOC in eddy-resolving simulations have been documented in the past. *Smith et al.* [2000] briefly discussed the AMOC stream function and the DWBC east of Abaco in their 1/10° POP (Parallel Ocean Program) model, and compared their results with limited transport measurements. *Saunders et al.* [2008] compared the vertical structure of the mean AMOC of *Smith et al.* [2000] and two other *z*-coordinate OGCMs to the results derived from hydrographic data near 26°N. They found the southward flowing limb of the modeled AMOC contained significantly more upper North Atlantic Deep Water (NADW) and less lower NADW than observed. Upper and lower NADW here refers to water in the approximate depth ranges 1000–3000 m and 3000–5000 m, respectively. The authors further point out that the discrepancy is linked to a typical mis-representation of the Nordic Seas Overflow

[1]Department of Marine Science, University of Southern Mississippi, Stennis Space Center, Mississippi, USA.
[2]Harte Research Institute, Texas A&M University-Corpus Christi, Corpus Christi, Texas, USA.
[3]Oceanography Division, Naval Research Laboratory, Stennis Space Center, Mississippi, USA.

0148-0227/12/2011JC007586

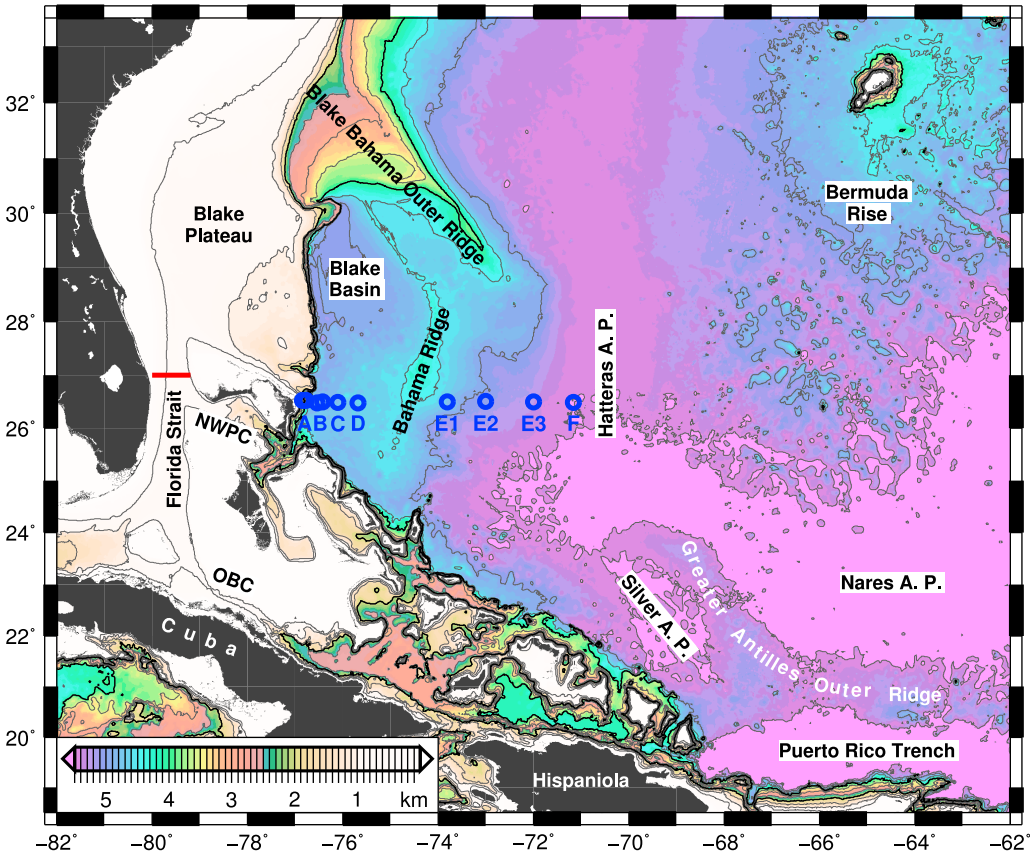

Figure 1. Bathymetry of the western subtropical North Atlantic. NWPC is Northwest Providence Channel, and OBC is Old Bahama Channel. The red line in the Florida Strait denotes the location of PEGASUS stations by *Leaman et al.* [1987]. Blues circles to the east of Abaco, Bahamas, denote the location of the current meter moorings summarized by *Bryden et al.* [2005b]. Locations A and B each have two mooring spots: A/A1 and B/B1.

Water (NSOW) in *z*-coordinate models. In the work by *Xu et al.* [2010], the modeled NSOW transports based on an eddy-resolving simulation are found to be in approximate agreement with long-term direct measurements in the Irminger and Iceland Basins. Their simulation used the Hybrid Coordinate Ocean Model (HYCOM [*Bleck*, 2002; *Chassignet et al.*, 2003]). *Hurlburt et al.* [2011] also show quite different structure of the AMOC stream function between several *z*- and layered models (e.g., HYCOM). These results call for a direct comparison between the AMOC in HYCOM simulations and the updated database along 26.5°N, one objective of this study.

[4] The purpose of the model-data comparisons, however, is not just to identify the strengths and shortcomings of the simulations. Observationally, there are questions that require further clarification. The mean observed AMOC transport in the upper 1000 m of the water column is 18.4 Sv; see section 2.1.1 and *Kanzow et al.* [2010] for a discussion on the first four years of the RAPID data. How does this transport compare to the 13 Sv AMOC contribution estimated in the FC by *Schmitz and Richardson* [1991] and what are the sources and water masses of this northward transport? Furthermore, the moored instrument array along 26.5°N in the western boundary of the subtropical North Atlantic is located in a region of complex bathymetry; see Figure 1 for detail. The general circulation pattern of the southward (AMOC) transport in this area is not well-known. Thus, the other objective of this study is to apply the model simulations (1) to clarify the contributions to and sources of the northward limb of the AMOC and (2) to explore the deep circulation pattern in the western subtropical North Atlantic. These applications yield a general consistency between the model results and available observations.

[5] The paper is organized as follows. After the introduction, the key observational results and model simulations are summarized in section 2. In section 3, the model-based, mean vertical structure of the trans-basin AMOC transports, the FC through the Florida Strait, and the western boundary currents east of Abaco are compared to the available observations. The model-determined deep circulation patterns in the western subtropical North Atlantic, compared to limited observations, are discussed in section 4. The summary and discussion follow in section 5.

2. Observations and Eddy-Resolving Simulations

2.1. Observations

[6] Several observational datasets have been collected along 26.5°N in the subtropical North Atlantic, including transports of the trans-basin AMOC and the western boundary currents through the Florida Strait and east of Abaco, Bahamas. These observations were designed for studying the

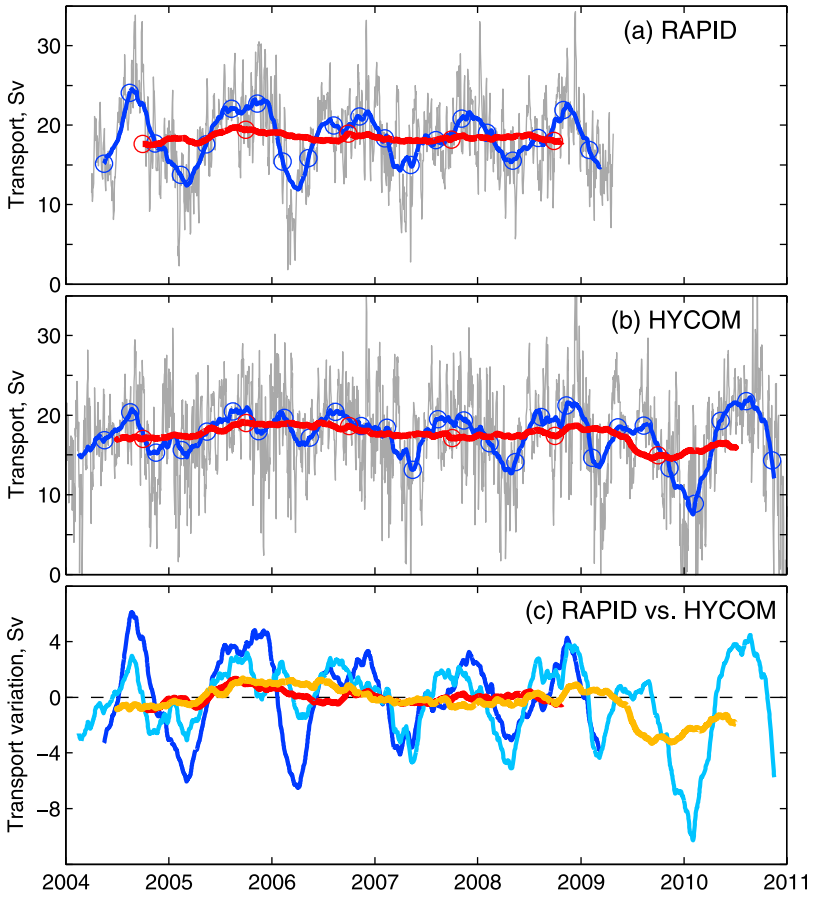

Figure 2. (a and b) Time series of the AMOC northward transport across 26.5°N based on the RAPID data over Apr. 2004–Apr. 2009 and HYCOM simulation E126 over 2004–2010. Gray lines are daily mean transports, blue and red lines for 3 and 12-month running averages. (c) Observed and modeled transport variations relative to the 5-year means over Apr. 2004–Apr. 2009: 18.4 Sv in the RAPID data and 17.8 Sv in the HYCOM simulation. Blue (RAPID) and light blue (HYCOM) lines denote 3-month running averages, red (RAPID) and orange (HYCOM) lines denote the 12-month running averages.

AMOC and related ocean currents at all depths. They are also the key datasets used in evaluating ocean model simulations of these features. If sufficiently realistic, the simulation can in turn help place the observations in a larger-scale context of the ocean circulation, which has been sparsely observed.

2.1.1. Transbasin AMOC Transport

[7] Since March 2004 the joint U.K.-U.S. Rapid Climate Change-MOC program has deployed a moored instrument array (RAPID array hereafter) along 26.5°N in the Atlantic to continuously measure the strength and vertical structure of the AMOC. The observational strategy for the RAPID array and results based on the first year of data are described by *Kanzow et al.* [2007] and *Cunningham et al.* [2007]. Figure 2a depicts a five-year time series of the AMOC transport based on the RAPID array over April 2004–April 2009, defined as the net transport above an observed overturning depth D_O of 1050 m (often simplified as 1000 m). D_O is the depth of maximum overturning based on the time averaged transport profile. The results reveal that the AMOC transport contains high variability on short timescales but much lower variability on annual and longer timescales. The daily mean transports have a wide range from about 2 to 34 Sv, with a mean and standard deviation of 18.4 ± 5.0 Sv. In contrast, the five yearly averaged transports range from 17.6 to 19.4 Sv and have a standard deviation of 0.7 Sv.

[8] Such a low variability of the yearly averaged AMOC transports is not continued in 2010, however. New RAPID results for 2010 suggest a yearly mean transport of about 14 Sv (a reviewer comment and consequent personal communication with W. E. Johns, University of Miami, 2011). Although the focus of this study is the time mean structure of the AMOC, it is interesting to compare how the variation of the AMOC transport is simulated in model. The modeled AMOC transport over 2004–2010, based on simulation E126 (see section 2.2), is shown in Figure 2b and the transport variations on seasonal and interannual scales are directly compared to the data in Figure 2c. The modeled seasonal variation in the first two and half years, probably in transition from climatological to interannual forcing, is significantly lower than observed. Starting in 2007, however, the modeled transport variations agree well with the data (Figure 2c). The model results also yield a significant transport decrease from 17.8 Sv over 2004–2009 to 14.9 Sv in 2010. An analysis of the model wind field suggests that the Ekman transport could account for about 2 Sv of the decrease. The abnormal wind in 2010 probably reflects the

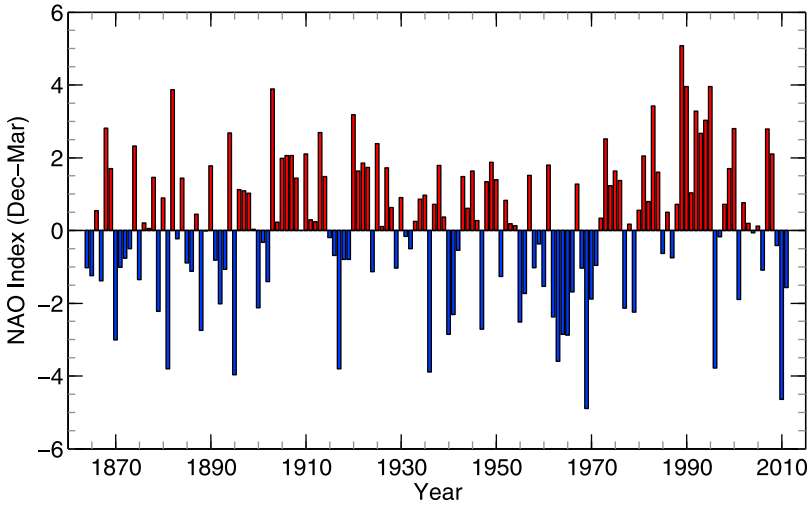

Figure 3. Winter (December through March) index of the North Atlantic Oscillation (NAO [*Hurrell*, 1995]) based on the difference of normalized sea level pressure between Lisbon, Portugal, and Stykkisholmur/Reykjavik, Iceland, since 1864. Positive values of the index indicate stronger-than-average westerlies over the middle latitudes. Data provided by the Climate Analysis Section, National Center for Atmospheric Research, Boulder, Colorado.

extremely nagative phase of the North Atlantic Oscillation (NAO [*Hurrell*, 1995]), with the lowest NAO index of the last four decades (Figure 3).

[9] The AMOC transport has also been estimated from occasional transatlantic hydrographic sections [e.g., *Roemmich*, 1980; *Hall and Bryden*, 1982; *Ganachaud and Wunsch*, 2000; *Lumpkin and Speer*, 2003; *Bryden et al.*, 2005a]. Figure 4 is used to compare the vertical profiles of the meridional transport per unit depth based on the RAPID data and the hydrographic sections of *Bryden et al.* [2005a]. The hydrographic results yield an AMOC transport of 18.6 Sv and a D_O of 1080 m, similar to 18.4 Sv and 1050 m from the RAPID data. However, the RAPID data yield more transport in the upper NADW and less in the lower NADW. The ratio between upper and lower NADW transports is 1.5 based on the RAPID data versus 1.1 based on the hydrographic data (Table 1). It is also noteworthy that the AMOC transports based on hydrographic sections contain various short-term variabilities. As shown by *Kanzow et al.* [2010], the aliasing of seasonal AMOC anomalies might have accounted for a large part of the 8 Sv long-term slowdown inferred by *Bryden et al.* [2005a].

2.1.2. Boundary Currents Through the Florida Strait and East of Abaco, Bahamas

[10] The FC has probably the best-established transport of any current in the world's oceans, in large part thanks to the well-defined boundaries of the Florida Strait and to the relatively low amplitude and benevolent frequency spectra of the fluctuations. The mean and standard deviation of the transport estimates at 27°N, based on over 300 shipboard sections and more than 25 years of daily cable observations, are 32.1 ± 3.3 Sv [*Meinen et al.*, 2010]. About 20% of the total variance is on interannual and longer timescales. In addition, the horizontal and vertical distributions of water properties and northward velocity across the FC are also relatively well-established [*Roemmich and Wunsch*, 1985; *Leaman et al.*, 1987]. Several investigators have partitioned the observed transport with temperature; see Table 2.

[11] The western boundary current east of Abaco has been measured by moored current meter arrays 7 times over 11 years from March 1986 to July 1997; see Figure 1 for mooring locations. This extensive database was summarized by *Bryden et al.* [2005b] and used to define the structure and the transport of the DWBC off Abaco and to estimate the transport of the recirculation offshore of the DWBC; see also *Lee et al.* [1990, 1996] for results based on early deployments. The mean DWBC exhibits a strong southward velocity core of about 16 cm s^{-1} at an offshore distance of about 55 km and extends out to about 160 km. The estimated mean DWBC transport is 34.6 Sv southward with an uncertainty of 3.7 Sv. These transport values are based on current meter time series with total record length of about five years. Offshore of the DWBC a broad, slow northward flow of deep water is observed. While the data coverage (both spatial and temporal) is substantially less for this northward recirculation, a transport of about 11 Sv is estimated using a space-time average of the measured currents [*Bryden et al.*, 2005b].

[12] The transports of the deep and shallow western boundary currents east of Abaco have also been studied using the RAPID array data collected during March 2004–May 2005 [*Johns et al.*, 2008]. Below about 1000 m, the yearly mean net transport within 500 km offshore of the Abaco coast is 26.5 Sv southward, which is divided nearly equally between 13.9 Sv upper NADW and 12.6 Sv lower NADW. These transport estimates generally agree with the results from moored current meter data [*Bryden et al.*, 2005b]. In the top 1000 m over 500 km off the Abaco coast, *Johns et al.* [2008] estimate a net northward transport of 6.0 Sv for the thermocline-intensified Antilles Current (AC hereafter), compared to near zero by *Bryden et al.* [2005b].

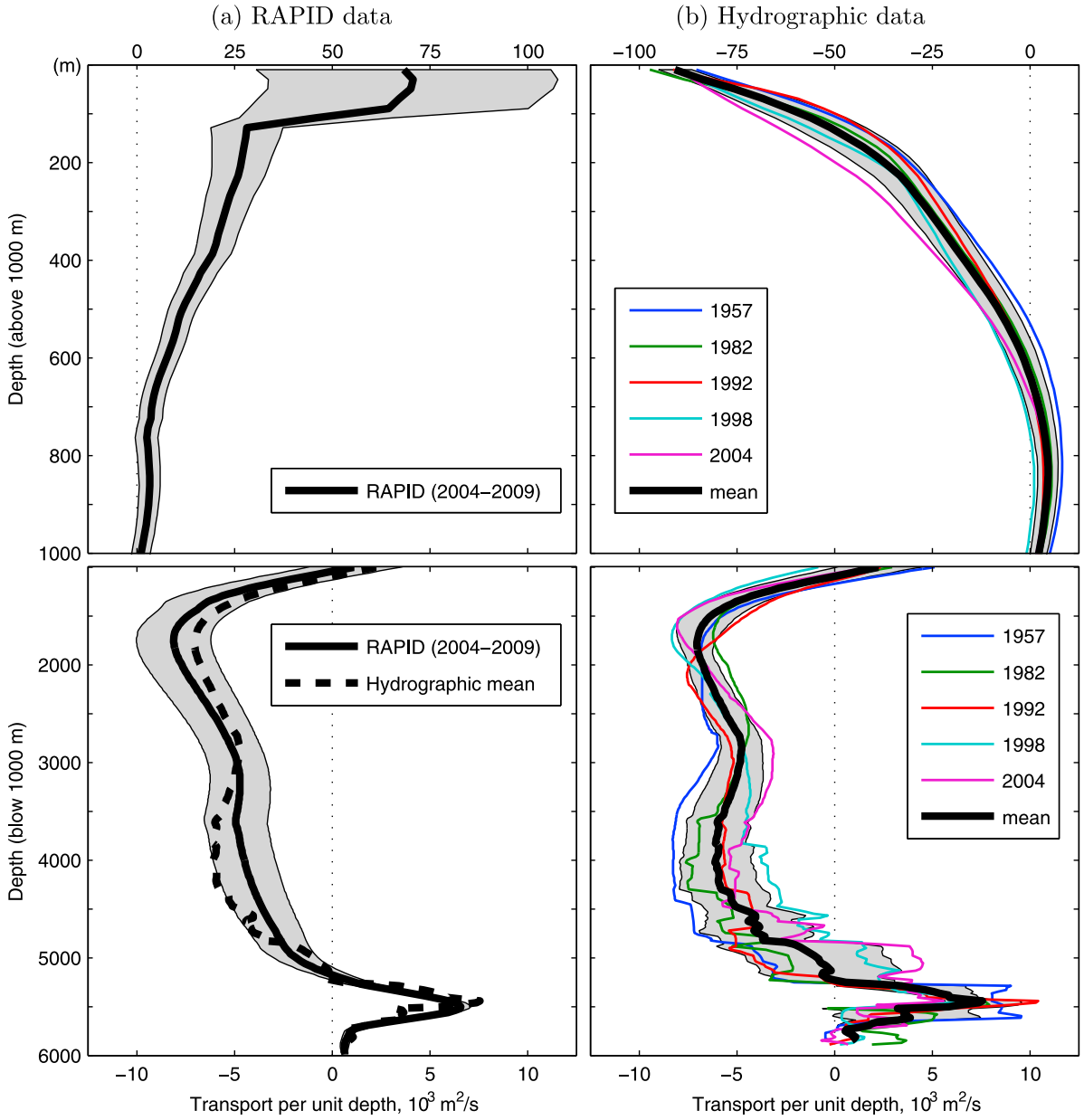

Figure 4. Zonally integrated meridional transport per unit depth in the water column above and below 1000 m based on (a) the five-year RAPID data and (b) the five hydrographic sections of *Bryden et al.* [2005a]. Thick solid lines and gray background denote the means and standard deviations. Thin colored lines in Figure 4b denote results of individual surveys. Note the hydrographic results are mid-ocean geostrophic transports, while the RAPID results in addition include the Florida Current and Ekman transports (both above 1000 m). Below 1000 m the mean hydrographic profile is overlaid as a dashed black line in Figure 4a for comparison.

2.2. Eddy-Resolving Atlantic Simulations Using HYCOM

[13] Results from three numerical experiments (E015, E026, and E126) are discussed in this study. These simulations have a horizontal resolution of 0.08° and 32 layers in the vertical. The computational domain extends meridionally from 28°S to the Fram Strait at 80°N. No inflow/outflow is prescribed at the northern and southern boundaries. Within a buffer zone of about 3° from the northern and southern boundaries, the model potential temperature (T) and salinity (S) are restored to a monthly ocean climatology, the Generalized Digital Environmental Model (GDEM [*Carnes*, 2009]), with an *e*-folding time of 5–60 days that increases with distance from the boundary. Simulations E015 and E026 were integrated with monthly climatological forcing from the European Center for Medium-Range Weather Forecasts reanalysis (ERA40 [*Uppala et al.*, 2005]). To better simulate the surface mixed layer, submonthly wind anomalies from the Fleet Numerical Meteorology and Oceanography Center 3-hourly, 0.5° Navy Operational Global Atmospheric

Table 1. Basin-Wide Mean Meridional Transport Near 26°N[a]

Depth Range	Hydrographic	RAPID	E126	E026	E015
$< D_O$	18.6	18.4	17.8	18.2	18.4
D_O - 3000	−10.7	−12.3	−13.3	−13.9	−14.3
3000 - D_R	−10.0	−8.3	−7.3	−6.9	−5.3
$> D_R$	2.1	2.2	2.8	2.6	1.2
D_O, m	1080	1050	1050	1000	1050
D_R, m	5230	5180	4800	4800	4800

[a]Units are in Sv, positive northward. D_O (overturning depth) and D_R (reversal depth) are defined as the depth of maximum and minimum transport from the time-averaged transport profile. Hydrographic results are based on five surveys [*Bryden et al.*, 2005a]. Results from the RAPID array and the HYCOM simulations are 5-year means (Apr. 2004–Apr. 2009 for E126; years 16–20 for E026 and E015).

Prediction System (NOGAPS [*Rosmond et al.*, 2002]) for the year 2003 are added to interpolated monthly means. The model results of E015 yielded NSOW transports that are approximately consistent with the estimates derived from a series of long-term moored current meter arrays in the Iceland and Irminger Basins [*Xu et al.*, 2010].

[14] Simulation E026 is designed to improve two aspects of the earlier model results. First, the results of E015 yield too little northward flow of Antarctic Bottom Water (AABW) across the Equator. This is in part due to the vertical resolution between NADW and AABW being too coarse. While E026 also has 32 layers, the lowest six layers have finer vertical resolution. The reference densities (σ_2, in kg m^{-3}) of the five deepest layers are 37.10, 37.17, 37.30, 37.42, 37.48 in E015 and 37.09, 37.11, 37.13, 37.15, 37.20 in E026. Second, the results of E015 generally show lower than observed eddy kinetic energy (EKE) in the deep Gulf Stream and the North Atlantic Current (NAC). To increase the EKE and eddy-driven recirculations in the deep ocean, the bottom drag coefficient C_D is set to 0.001 (0.0025 in E015). This change however is applied only after 10 years of integration due to an oversight. As a third change, E026 uses a new version of GDEM for initialization and buffer zone restoring. The new version includes many more T/S profiles, especially from Argo data, thus generally improving the ocean climatology. The difference, however, is not significant (M. Carnes, personal communication, 2010).

[15] Experiment E026 was integrated for 25 years (20 years for E015). A twin experiment, E126, is performed to explore the model sensitivity to surface forcing. The simulation is initialized from the results of E026 at the beginning of model year 16 and has the same configuration as E026, except that it uses interannual surface forcing from NOGAPS for years 2004 to 2010. To avoid new spin-up/down due to differences between ERA40 and NOGAPS, the long-term mean of NOGAPS wind-forcing is replaced with the mean of ERA40. The results of E126 reproduced some of the observed AMOC transport variations from the RAPID data (Figure 2).

[16] Selected measures of the modeled circulation as a function of integration time are presented in Figure 5. For simplicity, only results of an annual running mean are shown. The kinetic energy per unit mass averaged over the computational domain increases to about 34 and 32 cm^2 s^{-2} in E015 and E026 after 10 years of the model spin-up. The kinetic energy in E026 increases from 32 to 35 cm^2 s^{-2} from year 10 to 15 due to the C_D change and remains on that level thereafter. Interannual forcing in E126 also results in slightly higher energy and larger variation (Figure 5a). Throughout

Table 2. Florida Current Transport Broken Down Into Five Temperature (T) Ranges[a]

T Range (°C)	SR91	HB82	LJR89	HYCOM
>24	8.9	8.1	9.2	10.6
17–24	8.4	9.3	10.0	10.1
12–17	5.4	6.6	6.7	5.8
7–12	6.1	5.0	3.9	4.0
<7	–	0.5	–	0.3
Sum	28.8	29.5	29.8	30.8

[a]Units are in Sv. The transports of HB82 [*Hall and Bryden*, 1982] and LJR89 [*Leaman et al.*, 1989] are recalculated in SR91 [*Schmitz and Richardson*, 1991, Table 2]. Note the values in SR91 denote transport into the Caribbean Sea, while the values in HB82 and LJR89 denote transports through the Florida Strait near 26°N and 27°N, respectively. Thus flow through Northwest Providence Channel and Old Bahama Channel (Figure 1) could contribute to their transport differences. The FC transport values in HYCOM are from simulation E026 at 27°N.

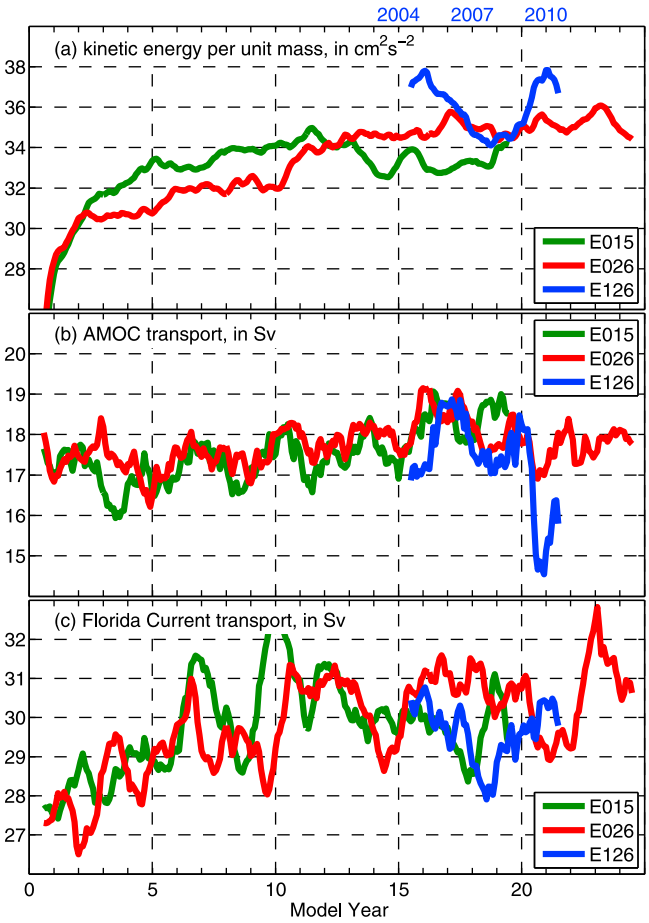

Figure 5. Time evolution of the model-based (a) kinetic energy per unit mass averaged over the computational domain, (b) trans-basin transport above 1000 m at 26.5°N, and (c) transport of the Florida Current at 27°N. Simulations E015 and E026 are integrated for 20 and 25 years, respectively; simulation E126 is integrated over 2004–2010. Results are based on 12-month running averages of the monthly means.

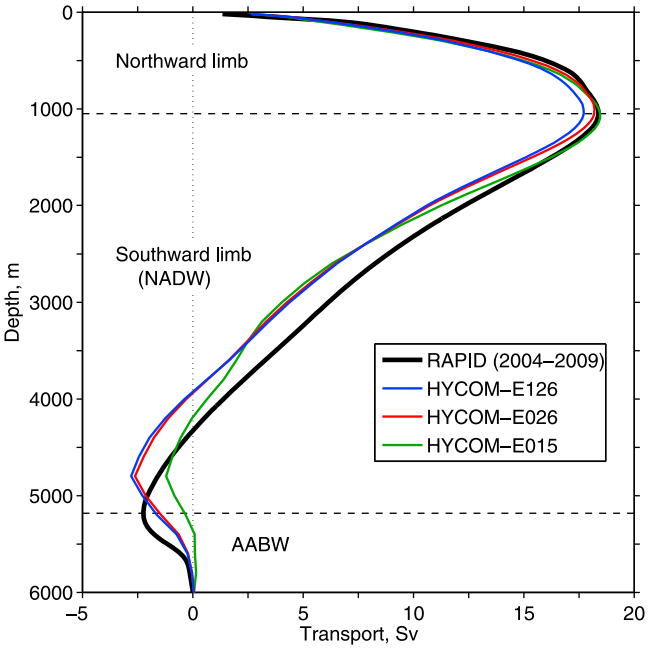

Figure 6. Net transport (in Sv) across the Atlantic at 26.5°N accumulated from surface to bottom. The black line denotes a 5-year mean profile based on the RAPID data (Apr. 2004–Apr. 2009). Colored lines are 5-year mean profiles from three 0.08° HYCOM simulations (model years 16–20 for E015 and E026; Apr. 2004–Apr. 2009 for E126). Horizontal dashed lines denote the observed overturning depth (D_O) at 1050 m and reversal depth (D_R) at 5180 m.

the integration of E015 and E026, the annual mean AMOC transports across 26.5°N (Figure 5b) are relatively stable, despite much larger variations on short timescales. As mentioned, the yearly averaged AMOC transports in E126 are relatively stable over 2004–2009, but decrease significantly in 2010. For E015 and E026, the annual mean transports of the FC (Figure 5c) exhibit a gradual increase to about 30 Sv in the first 10 years of integration, implying the spin-up of the wind-driven subtropical gyre, then remain relatively stable on long-term scales thereafter. Overall, although an integration of 20–25 years might be much too short for an OGCM to reach an equilibrium state, the simulation after 10–15 years has spun-up to a state of relatively stable domain-wide mean kinetic energy, cross-basin AMOC transport, and key currents like the FC. There are still variations on the interannual scale, even in E015 and E026. Therefore, a five-year average (years 16–20 for E015 and E026; Apr. 2004–Apr. 2009 for E126) is selected as the model mean state for further discussion. The results of E026 over years 21 to 25 are very similar to years 16–20.

3. Time Mean Model-Based AMOC

[17] So how does the model-based mean AMOC compare to the observations? And what do the model results suggest for the sources of the northward AMOC transport? To answer these questions we need to examine several aspects of the modeled AMOC, including the vertical structure of the cross-basin meridional transport and its western boundary current components, i.e., the FC through the Florida Strait and the DWBC east of Abaco. The reasons for focusing on the mean structure in this study are, first, the AMOC transport observed at this latitude exhibits a much lower variability on longer timescales than on shorter timescales; second, the model's ability to accurately simulate the observed mean AMOC structure, including transports of various water masses in both the northward and southward limb of the AMOC, is critical for using the model results to understand how the AMOC operates and to predict how it will change.

3.1. Zonally Integrated, Vertical Profiles of Meridional Overturning

[18] Figure 6 depicts the five-year mean, net cross-basin transport at 26.5°N cumulative from surface to bottom. The RAPID data yield a northward AMOC transport of 18.4 Sv above (D_O) 1050 m, a southward NADW transport of 20.6 Sv that extends from 1050 m to a depth of reversal (D_R) at 5180 m, and further below a northward AABW transport of 2.2 Sv. Both E015 and E026 reproduce the AMOC transport and D_O accurately (Table 1) and the use of interannual forcing has little impact on the vertical structure. Although the overall structure is similar in the models and the data, below 1000 m all simulations yield a transport profile that is shallower than observed by as much as 400 m. Another approach to quantifying the structure difference is to divide the NADW transport into upper and lower NADW [*Saunders et al.*, 2008]. The ratio of the upper and lower NADW transports is 2.7 in E015, 2.0 in E026, and 1.8 in E126, compared to 1.5 based on the RAPID data (Table 1). More consistent results are found in E026 and E126, which have a better representation of the northward AABW transport across the Equator than E015, highlighting the fact that the lower NADW is influenced by a contribution from AABW. Otherwise, the results of E015 and E026 are similar and the latter, sometimes including results from E126, are used for primary discussion hereafter.

[19] One might wonder why the vertical structure of the transport profile below 1000 m is important to the AMOC. The structure is important because it directly impacts the AMOC associated meridional heat flux. Also, the transports at different depths represent contributions of different origin. As illustrated in Figure 7a, the observed southward transport per unit depth below 1000 m contains a main maximum centered at 1500–2000 m and a weaker, secondary maximum centered near 4000 m. Tracer data, collected in the hydrographic surveys at this latitude (not shown), indicate that these two maxima are connected with the contributions from Labrador Seawater (LSW) and NSOW, respectively. To examine how well this observed transport structure is represented in current eddy-resolving models, we compare the RAPID transport profile with those from three HYCOM simulations and two additional model profiles derived from two other widely used, state-of-the-art OGCMs (Figure 7a). The 1/10° POP results are representative of three OGCMs discussed by *Saunders et al.* [2008]. Results from 1/12° NEMO (Nucleus for European Modeling of the Ocean) were included in the work by *Hurlburt et al.* [2011], which focused on the Gulf Stream pathway in relation to the deep circulation and the AMOC. All simulations, regardless of model formulation and configuration, yield a stronger than

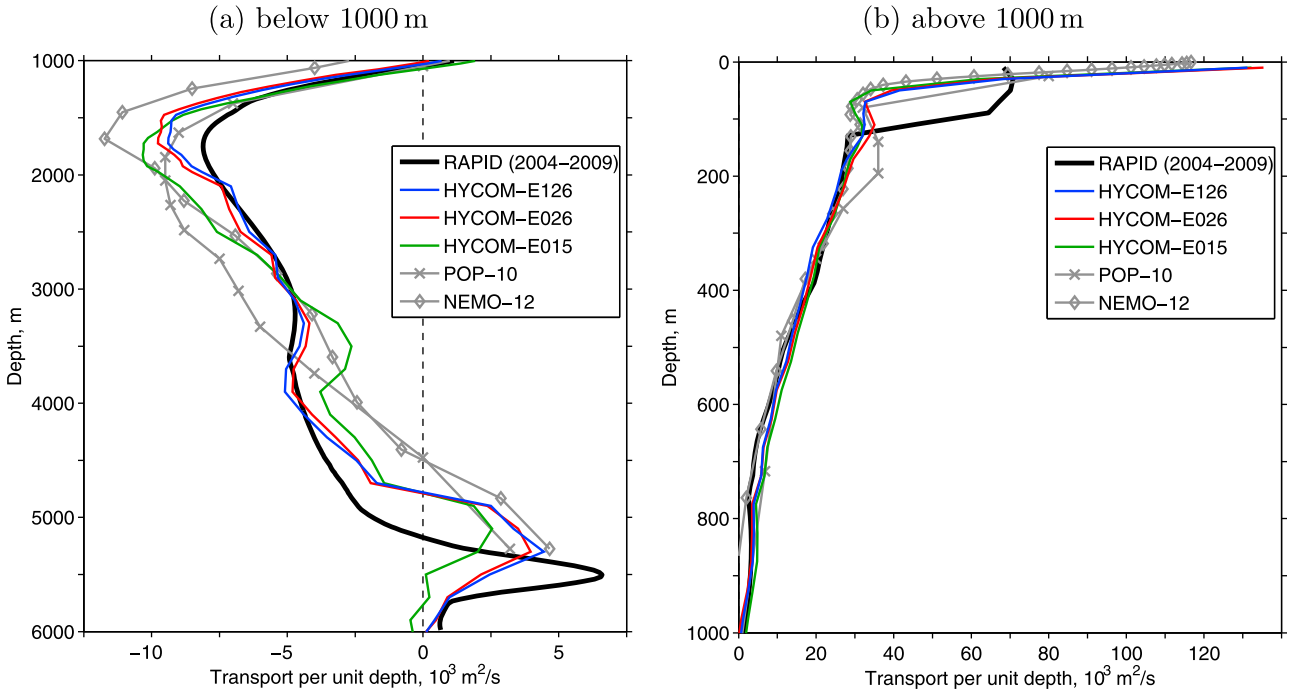

Figure 7. Net transport per unit depth (in 10^3 m^2 s^{-1}) across the Atlantic at 26.5°N. The black line denotes a 5-year mean profile based on the RAPID data. Colored lines are 5-year mean profiles from three 0.08° HYCOM simulations (model years 16–20 for E015 and E026; Apr. 2004–Apr. 2009 for E126). Gray lines with crosses and diamonds are results from two *z*-coordinate OGCMs: 1/10° POP and 1/12° NEMO. The POP results have been discussed by *Saunders et al.* [2008]. Results from the NEMO simulation are discussed by *Hurlburt et al.* [2011].

observed transport maximum for LSW, but only the HYCOM simulations yield a secondary transport maximum near 4000 m corresponding to NSOW. Therefore, although the modeled southward limb of the AMOC in HYCOM exhibits a shallow bias, the contributions of LSW and NSOW at different depths are approximately consistent with data.

[20] Above 1000 m the modeled transport structure is generally similar to observations (Figure 7b). The main difference is in the top 100 m, where the modeled profiles, including POP and NEMO, are more strongly intensified near the surface than the RAPID data. This difference occurs because the Ekman transport is assumed to be evenly distributed over the top 100 m of the RAPID profile; note the high deviation above 100 m in Figure 4a. In Figure 8 the modeled mid-ocean transport, calculated as a direct integration of the modeled meridional transport from Abaco, Bahamas to Africa, is compared to the mean geostrophic transport based on hydrographic sections and a mean Ekman transport of 3.2 Sv based on the model wind. The Ekman transports in Figure 8 are assumed to decrease linearly from their value at the surface to zero at 50 m [*Hall and Bryden*, 1982]. The model results are consistent with the sum of geostrophic transport and Ekman transport that decreases with depth. Between about 600 m and 1000 m, both model and geostrophic results suggest weak northward flow: 0.9 Sv in E026 and 1.3 Sv from the geostrophic results (see also Figure 4b). This transport represents a small contribution from modified/upper Antarctic Intermediate Water (AAIW) to the AMOC through the mid-ocean. Thus the mid-ocean (Ekman and AAIW) contributes 4.1 out of the 18.2 Sv

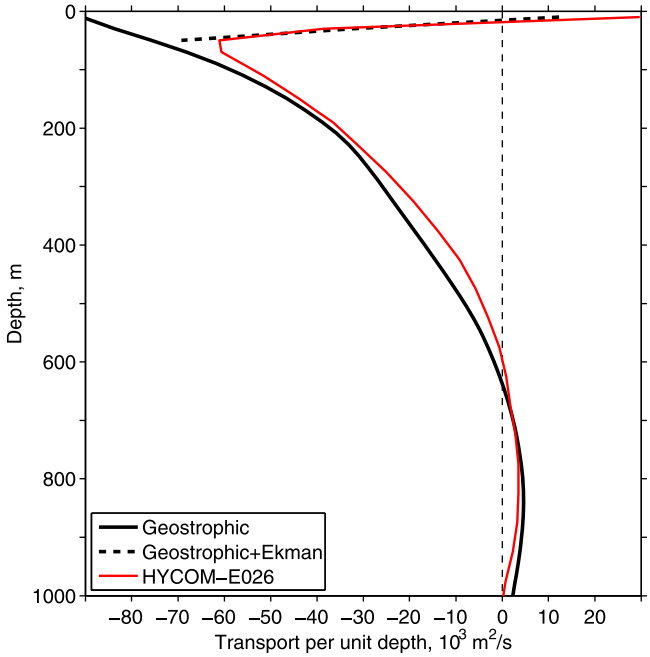

Figure 8. Net transport per unit depth (in 10^3 m^2 s^{-1}) across the Atlantic at 26.5°N, exclusive of the Florida Strait. The solid black line denotes the mean geostrophic transport per unit depth based on the work of *Bryden et al.* [2005a], while the dashed black line denotes the sum of geostrophic and Ekman transports in the top 50 m. Model results are based on a 5-year mean from E026 (model years 16–20).

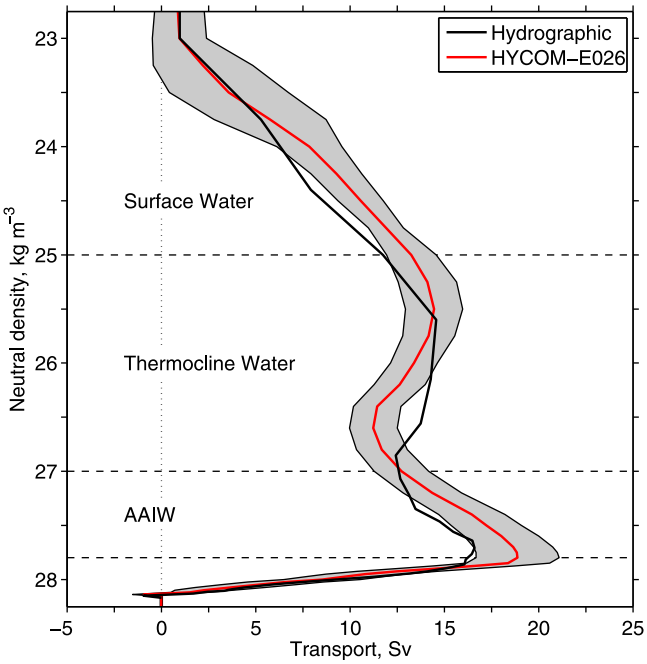

Figure 9. Net transport (in Sv) across the Atlantic along 26.5°N in neutral density space, accumulated from surface to bottom. The thick black line is the observational profile based on an inverse study using a 1992 hydrographic section [*Lumpkin and Speer*, 2003]. Red line and gray background are the mean and standard deviation of the model results, based on monthly mean profiles from E026 for model years 16–20.

modeled AMOC transport in E026. The remaining 14.1 Sv flow through the Florida Strait, consistent with the 13 Sv AMOC contribution estimated by *Schmitz and Richardson* [1991].

[21] To clarify the water masses of the northward limb of the AMOC, we calculate the trans-basin transports in neutral density γ^n space (Figure 9). This calculation requires information on zonal distributions of the transport and density, which is not available from the RAPID data. An inverse result by *Lumpkin and Speer* [2003] based on a 1992 hydrographic section is included for comparison. The basic structure agrees despite some differences in detail between the model and inverse results. Both exhibit a maximum overturning transport (18.9 Sv in E026) at γ^n of about 27.8 kg m^{-3}. Above this isopycnal the flows are overall northward. However, a layer of weak southward flow exists both in the model and inverse results. This embedded "shallow overturning" occurs because the southward return flow in the horizontal subtropical gyre is slightly denser than its northward counterpart. Using a simplified water mass classification of the western North Atlantic [e.g., *Joyce et al.*, 2001; *Hall et al.*, 2004], the modeled northward transport is broken down into three layers: 13.2 Sv surface water (γ^n < 25 kg m^{-3}), −0.5 Sv thermocline water (25–27 kg m^{-3}), and 6.2 Sv AAIW (27–27.8 kg m^{-3}). The northward limb of the AMOC, therefore, consists of about 2/3 surface water and 1/3 AAIW. The thermocline water in between circulates within the subtropical gyre and does not contribute to the AMOC.

3.2. Florida Current at 27°N

[22] The FC carries water from both the North Atlantic subtropical wind-driven gyre and the upper limb of the AMOC [*Schmitz and Richardson*, 1991]. As a key measure of both circulation patterns, it is necessary that the modeled FC has not only a realistic total transport, but also velocity and water property distributions across the Strait that are approximately consistent with observations.

[23] The five-year mean transport through the Florida Strait at 27°N is 30.8 Sv in E026 (Figure 5c), compared to an observed long-term mean of 32.1 Sv [*Meinen et al.*, 2010]. The modeled transport at this latitude is fed from three sources: (1) an eastward transport of 28.3 Sv at 81°W between Cuba and the southern tip of Florida, similar to the total Atlantic inflow of about 28 Sv into the Caribbean Sea [*Johns et al.*, 2002]; (2) a westward transport of 3.1 Sv through the Northwest Providence Channel (NWPC, Figure 1 for location), which is slightly stronger than the observed range of 1.2–2.5 Sv [*Richardson and Finlen*, 1967; *Leaman et al.*, 1995]; and (3) an eastward transport of 0.6 Sv through the Old Bahama Channel (OBC), opposite to a westward transport of about 2 Sv [*Atkinson et al.*, 1995]. The uncertainty for the last observed value is high [*Meinen et al.*, 2010]. These results indicate that the flow through the NWPC and OBC are the primary sources of the difference between observed and modeled FC transports at 27°N. The five years of daily mean FC transports from E026 have a standard deviation of 2.5 Sv, also lower than the 3.3 Sv observed [*Meinen et al.*, 2010]. This is due to climatological forcing. Results of E126 yield a standard deviation of 3.2 Sv.

[24] Cross-sections of the mean and standard deviation of the northward velocity at 27°N are illustrated in Figure 10. The observations, adapted from *Leaman et al.* [1987], were obtained by PEGASUS acoustic current profilers in a two-year field experiment. The modeled mean velocity, including the overall structure and the maximum value (188 cm s^{-1}), is in close agreement with observations. The standard deviation of the modeled velocity also depicts a distribution that is similar to observations, with a maximum on the western side of the Strait. The magnitude of the standard deviation, however, is substantially lower. Interannual forcing explains part of the difference. The maximum standard deviation is 36 cm s^{-1} in E126. As might be expected, the observed maximum is co-located with a high gradient in the mean velocity, and is generally associated with zonal shifts in the high velocity core. Zonal shifts at spatial scales smaller than the model resolution (about 8 km at 27°N) are not included, which is particularly relevant to the model versus observed variability adjacent to the western boundary. A similarly configured simulation, with the same climatological forcing but doubled resolution (not shown), yields elevated standard deviations exceeding 40 cm s^{-1} near the western side of the Strait and about 12 cm s^{-1} in the deepest part of the Strait.

[25] Distributions of mean T and S along 27°N are shown in Figure 11. The observations are based on 154 CTD profiles over 1982–2007 collected in the World Ocean Database. The observed S maximum (>36.6 psu) on the eastern side of the strait is associated with subtropical underwater. At the base of this S maximum there is water with T of 17.9–18.2°C and S of 36.4–36.6 psu. Both of these components

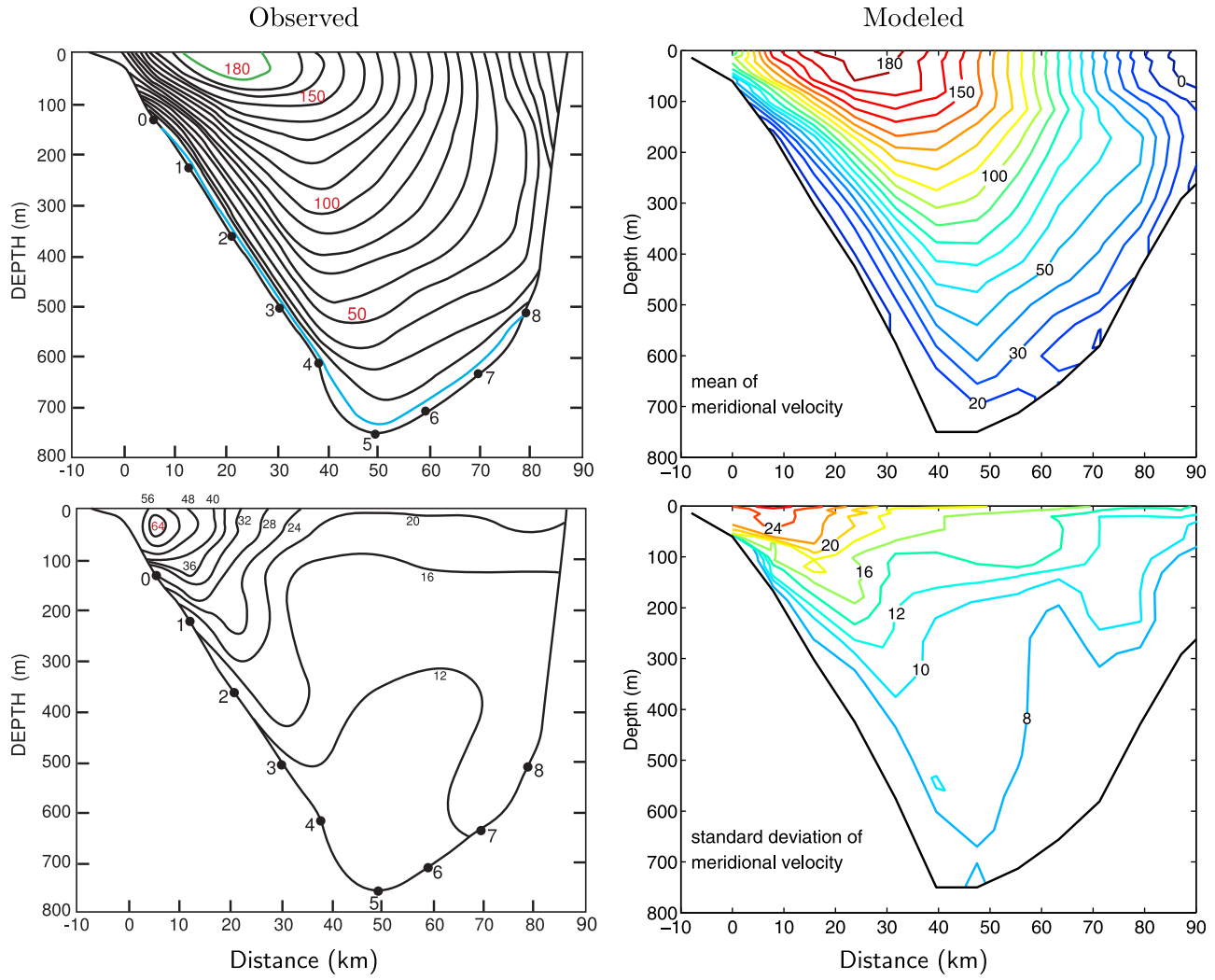

Figure 10. Vertical distribution of the meridional velocity (in cm s^{-1}) across the Florida Strait at 27°N: (top) mean and (bottom) standard deviation. The observed cross-sections are adapted from *Leaman et al.* [1987]. Model results are based on simulation E026 (years 18–20).

originate in the North Atlantic subtropical gyre. Above and below this saline water are layers of relatively fresh water from the South Atlantic. One is the near surface water, with T > 25°C and S < 36.4 psu. The other is the upper AAIW above the sill and over the deep western slope, with T < 12°C and S < 35.2 psu. While the values of the observed and modeled S maximum/minima differ by about 0.1 psu, the overall structure of the S distribution is essentially the same. These results indicate that the sources of the modeled FC are consistent with observations.

[26] To quantify the AMOC and North Atlantic subtropical gyre contributions, the modeled FC transport at 27°N is broken down into five T ranges in Table 2. *Schmitz and Richardson* [1991] estimated that the AMOC contribution consists of 7.1 Sv warmer than 24°C, 0.8 Sv in the range 12–24°C, and 5 Sv colder than 12°C. For the same ranges, the model results yield 8.5, 1.3, and 4.3 Sv, respectively. Thus, this analysis indicates that about 45% of the simulated FC transport at 27°N in HYCOM E026 is from the AMOC, primarily water with T > 24°C or T < 12°C. The remaining 55%, primarily thermocline water, is part of the western boundary current for the subtropical gyre.

3.3. Western Boundary Currents East of Abaco, Bahamas

[27] While the FC carries much of the transport for the northward limb of the AMOC, the DWBC to the east of Abaco, Bahamas is the known conduit for the southward limb of the AMOC at this latitude, carrying the recently ventilated NSOW and LSW southward from the north. Above the DWBC, the AC flows northward, mainly carrying water from part of the subtropical gyre that does not flow into the Florida Strait.

[28] Figures 12 and 13 depict the distribution of the mean meridional velocity east of Abaco and mean profiles at each mooring location. The observations are from *Bryden et al.* [2005b, Figure 4 and Table 1] and the model results are based on a mean of years 16–20 from simulation E026. The most basic structure of the flow field is in reasonable agreement, including the location and magnitude of the DWBC and AC along the boundary and their recirculations/

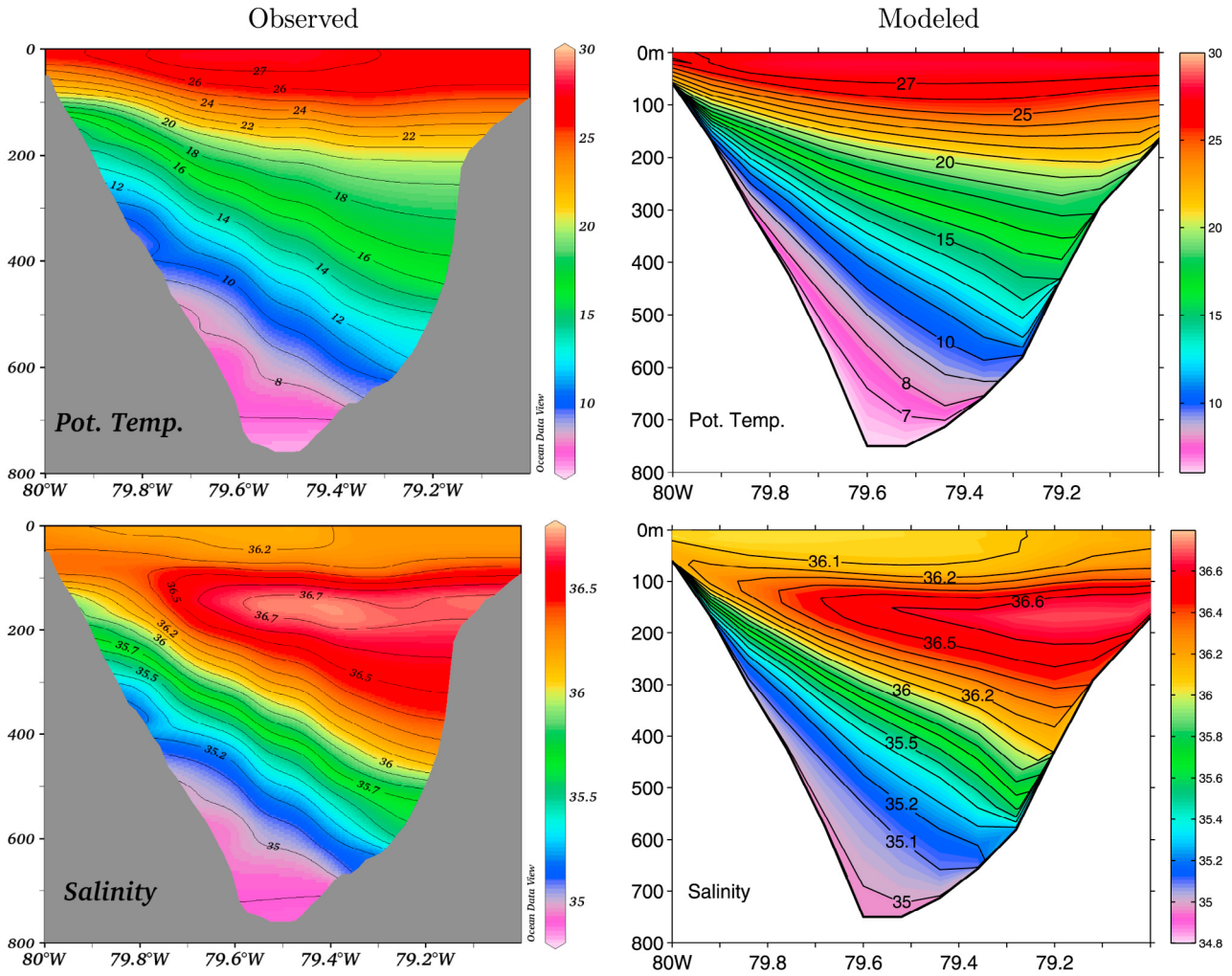

Figure 11. Distribution of mean potential temperature and salinity across the Florida Current at 27°N. The observed cross-section is based on CTD profiles over 1982–2007 available in world ocean database. The model results are based on a 5-year mean from simulation E026 (years 16–20).

return flows offshore. The modeled AC is wider than observed (180 vs. 130 km) and has higher core velocities (38 vs. 30 cm s^{-1}). In contrast, the modeled DWBC is narrower than observed (130 vs. 170 km) and has slightly higher maximum speeds (18 vs. 16 cm s^{-1} at moorings B/B1 in Figure 13). Offshore of the DWBC, the model results yield two northward recirculation flow patterns that are similar to observations. One is centered around 1500–2000 m depth near moorings E1 and E2, the other below 3000 m near mooring F. Note that the moorings are not evenly distributed and there is a 186 km wide gap above the Bahama Ridge (between moorings D and E1). The "observed" flow therein is a result of both extrapolation and interpolation; see *Bryden et al.* [2005b, p. 39] for details. Over the western and eastern slopes of the Ridge, the model results yield northward and southward flow, respectively. This flow pattern is found in both E026 and E126 and is discussed in the context of the regional and large-scale circulation in section 4. A similar regional abyssal circulation is also found in the high-resolution simulations of *Hurlburt and Hogan* [2000, section 7].

[29] The transport corresponding to the mean velocity structure in Figure 12 is shown in Figure 14. Above 1000 m the modeled AC transports 13.5 Sv within 180 km east of Abaco, and the net transport over a distance of 500 km is 8.6 Sv northward (9.5 Sv in E126), compared to a net transport of 6 Sv estimated by *Johns et al.* [2008] and near zero (over 625 km) by *Bryden et al.* [2005b]. The dynamic height measurements of *Johns et al.* [2008] allow only zonally integrated estimates, but have the advantage of requiring no spatial interpolation, compared to *Bryden et al.* [2005b]. A higher than observed AC transport is typical in OGCMs; see *Lee et al.* [1996, Table 2] for an example, although some model results are in agreement with observations [*Johns et al.*, 2002]. However, it is noteworthy that the AC is primarily part of the subtropical gyre and that its transport has little direct impact on the AMOC picture.

[30] Below 1000 m the modeled DWBC reaches a maximum mean transport of 30.4 Sv at 130 km (mooring D), similar to the data-based transport at same location. The latter however continues to accumulate to nearly 35 Sv at about 200 km (Figure 14). Although flow at mooring D is southward in the data, while close to zero in the model (Figure 13), part of this increase is probably due to the extrapolated/interpolated flow between moorings D and E1

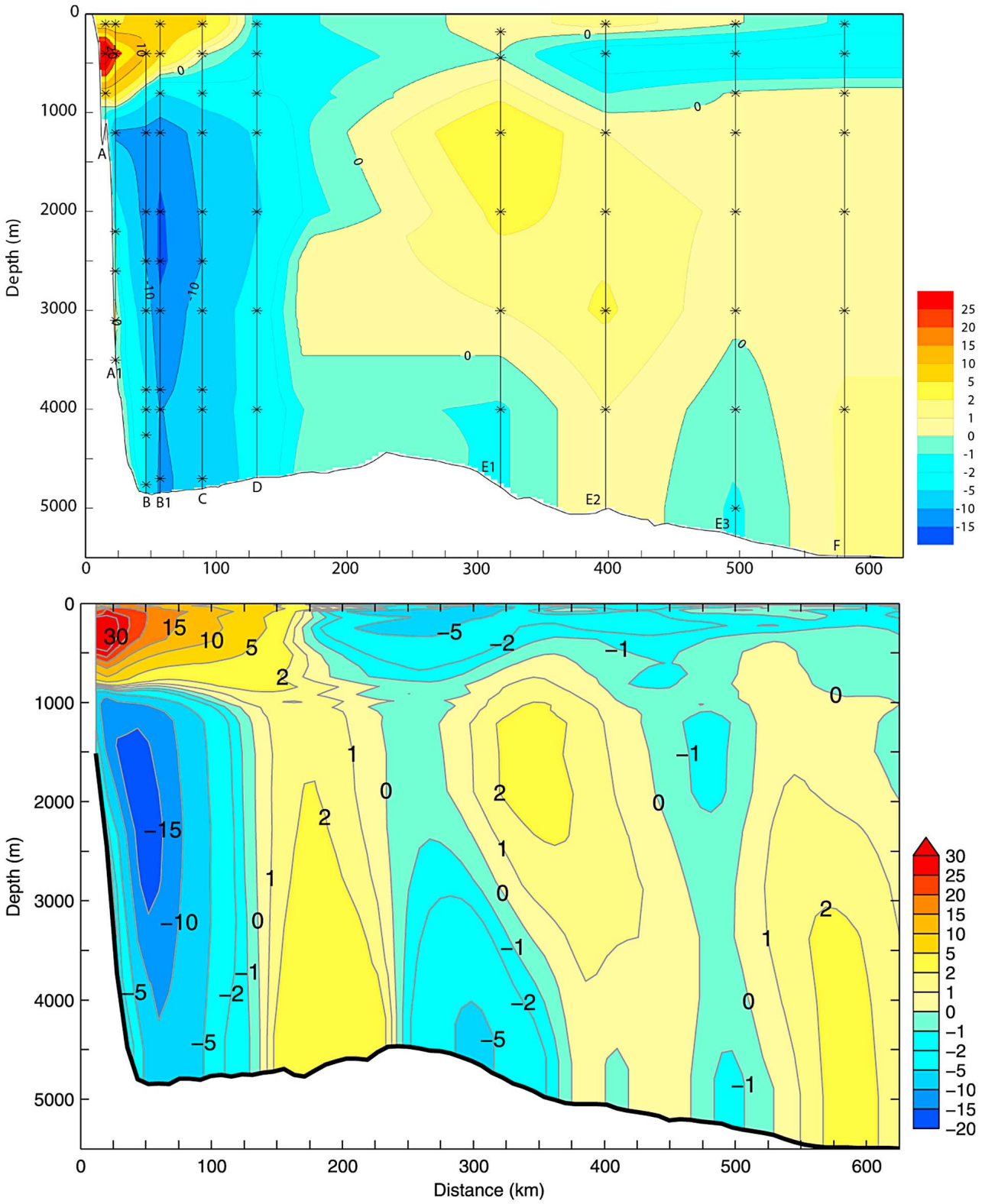

Figure 12. Comparison of mean meridional velocity (cm s^{-1}) in the western boundary current east of Abaco, Bahamas. The top plot, from *Bryden et al.* [2005b, Figure 4], is based on moored current meter arrays. The bottom plot is based on a 5-year mean from simulation E026 (years 16–20).

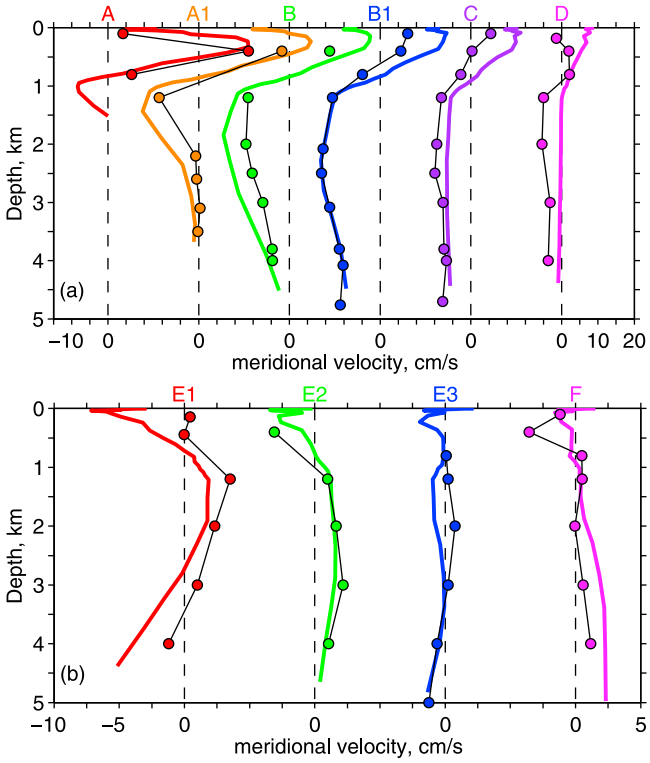

Figure 13. Comparison of the modeled mean meridional velocity profiles (solid lines) with historical moored current meter data (dots) east of Abaco: (a) moorings A, A1, B, B1, C, and D; (b) moorings E1-3, and F. Data are from *Bryden et al.* [2005b, Table 1]. Model results are based on a 5-year mean from simulation E026 (years 16–20).

(Figure 12). Farther east both the modeled and observed transports generally decrease due to northward recirculation (s). Within 500 km east of Abaco (77–72°W), the model results yield a net southward transport of 25.3 Sv, similar to 26.5 Sv of *Johns et al.* [2008]. The vertical structure of the modeled net transport, as illustrated in Figure 15, is also in reasonable agreement with the observations. The transport ratio between upper and lower NADW is 1.3 in E026 (1.2 in E126), compared to 1.1 in the work by *Johns et al.* [2008]. Interestingly, the modeled net transport over 500 km is also similar to that of *Bryden et al.* [2005b], despite large differences over the Bahama Ridge. Over the Hatteras Abyssal Plain (72–70°W), both model and observations show a northward flow, but stronger in model (Figures 13 and 14). East of 70°W (not shown), the model results exhibit some weak southward and northward flows below 1000 m, with a net northward transport of about 1 Sv.

4. Deep Circulation in the Western Subtropical North Atlantic

[31] The mooring arrays along 26.5°N have provided valuable meridional transport estimates at this latitude. In this section we investigate the simulated deep circulation pattern in the western subtropical North Atlantic that circumscribes the arrays. The area of interest is characterized by complex bathymetry (Figure 1), which should play a strong role in steering the deep flow. One prominent topographic feature is the Blake Bahama Outer Ridge (BBOR), which extends from the Blake Escarpment into the Hatteras Abyssal Plain at a depth range of 2000–5000 m. A secondary ridge, the Bahama Ridge, is located southwest of the BBOR at ~4500 m depth. In combination, these two ridges separate the Blake Basin (~5000 m) from the Hatteras Abyssal Plain (>5400 m). East of 69°W the depth decreases again over the western slope of the Bermuda Rise, shaping the Hatteras Abyssal Plain as a meridional "trough" centered along ~71°W. To the south there is another deep ridge at ~5200 m, the Greater Antilles Outer Ridge (GAOR), separating the Silver Abyssal Plain, the Neras Abyssal Plain, and the Puerto Rico Trench.

[32] The modeled mean circulation in the western subtropical North Atlantic is illustrated in Figure 16. The plotted vectors are transport per unit width, in $m^2\ s^{-1}$, for model layers 19–26 (Figure 16a) and layers 27 to the bottom (Figure 16b), roughly representing the upper and lower NADW, respectively. The results shown are from years 16 to 20 of E026, but similar circulation patterns are found from years 21 to 25, and in E126 over years 2004 to 2009. A continuous DWBC flows along the boundary in the layer containing upper NADW (Figure 16a): westward over south face of the BBOR, southward and southeastward along the Blake and Bahamas Escarpments, and eastward through the Puerto Rico Trench. Near 74°W, 23°N and 73°W, 22°N, part of the water branches off the mainstream of the DWBC and flows through the deep trench north of Hispaniola and the southern part of Cuba, before remerging in the Puerto

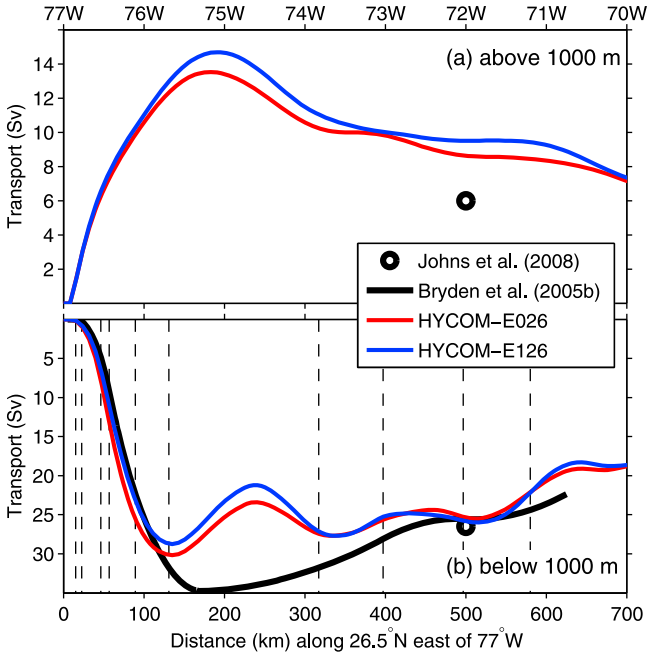

Figure 14. Volume transports accumulated eastward from the coast of Abaco, Bahamas: (a) above 1000 m and (b) below 1000 m. Model results are based on a 5-year mean of simulations E026 (years 16–20) and E0126 (Apr. 2004–Apr. 2009). Black circles are net transports over a distance of 500 km from *Johns et al.* [2008]. The black line in Figure 14b, from *Bryden et al.* [2005b, Figure 7], is transport based on moored current meter arrays. The vertical dashed lines denote the mooring locations.

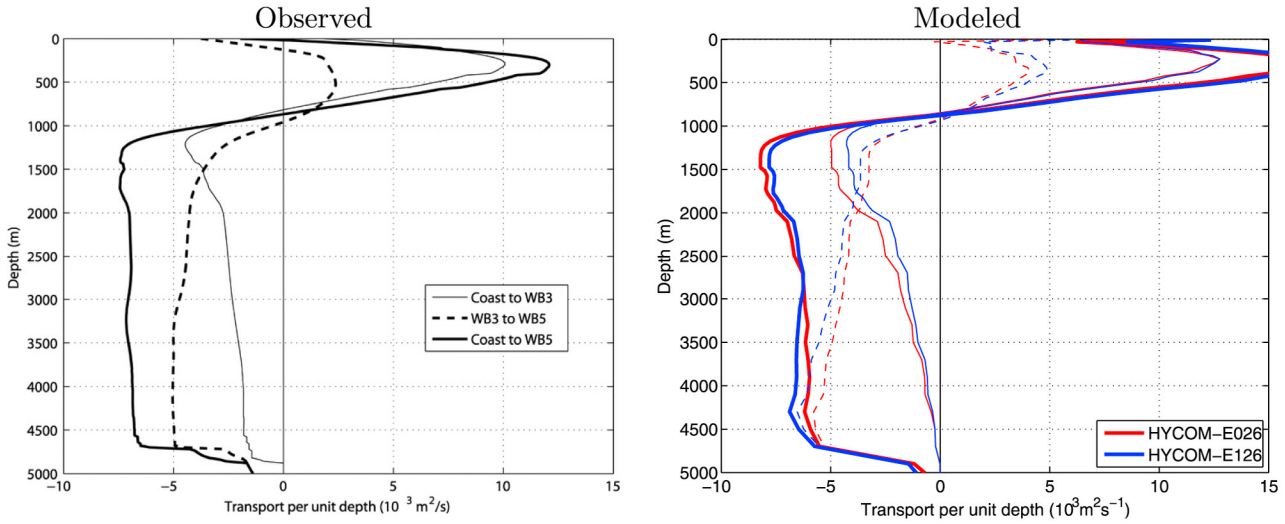

Figure 15. Mean meridional transport profile in the western boundary current within 500 km east of Abaco. Observational profiles, based on RAPID data, are from *Johns et al.* [2008, Figure 12]. Mooring locations WB3 and WB5 are about 50 km and 500 km east of Abaco. Model results are based on a 5-year mean of simulations E026 (years 16–20) and E126 (Apr. 2004–Apr. 2009).

Rico Trench. Several cyclonic recirculation gyres are found offshore of the DWBC, labeled A–D in Figure 16a. Gyre A is enclosed within the deep Blake Basin, similar to the cyclonic pattern inferred by *Amos et al.* [1971]. Gyre B is slanted northwestward over the southern end of the Bahama Ridge. A similar gyre is derived by *Johns et al.* [1997, Figure 11], based on a shipboard survey during June–July 1990, but is located slightly more offshore. The exact shape, size, or location of gyre B is critical for the velocity over the western slope of the Bahama Ridge (Figure 12) and the velocity difference at mooring D (Figure 13) might be explained by this gyre in the model being too inshore. Gyres B–D are to some extent connected, and their offshore portions form a continuous northward flow between about 20°N and 30°N. This northward flow is observed at the mooring locations E1 and E2 (Figures 12 and 13).

[33] The circulation pattern in the lower NADW layer is more complex (Figure 16b), reflecting stronger topographic steering. There are two branches of the southward DWBC in the vicinity of the BBOR and the Bahama Ridge. One branch flows westward into the Blake Basin over the BBOR along depth contours of 3500–4000 m. This branch continues southward along the Blake Escarpment similar to the DWBC in the upper NADW layer. There is also a closed cyclonic gyre A in the Blake Basin with roughly the same location/size as in Figure 16a. The other branch flows around the BBOR along the 4500–5000 m depth contours and continues southward along the eastern flank of the Bahama Ridge. A similar deep southward flow is observed at mooring location E1. These two branches merge east of Abaco and flow southeastward along the Bahamas Escarpment. Part of this merged DWBC continues to flow eastward into the Puerto Rico Trench. The majority of the flow, however, turns northwestward in the Silver Abyssal Plain and splits again near the northwest end of the GAOR. One branch continues to meander northward through the Hatteras Abyssal Plain, similar to flow observed at mooring location F along 26.5°N. The other branch turns clockwise around the GAOR and flows southeastward/eastward along the eastern/northern flank of the ridge. A similar flow pattern around the GAOR has been inferred by *Tucholke et al.* [1973, Figure 6], based on hydrographic stations, short-term current meter measurements, and bottom photographs.

5. Summary and Discussion

[34] The AMOC, responsible for about 1/4 the total heat transport of the global ocean and atmosphere, is an important element of the Earth's climate system. A data-based description of the mean strength and vertical structure of the AMOC has been relatively well-established along 26.5°N in the Atlantic. The five-year RAPID array data suggest that the AMOC transport at this latitude contains high short-term variability, but significantly lower variability on timescales longer than a year. Here we have used this database and other current measurements to examine the time mean AMOC in a climatologically forced, eddy-resolving Atlantic simulation using HYCOM. The model-based results are then used help to clarify the different contributions and sources of the northward transport and to explore the circulation patterns of the southward transport in the western subtropical North Atlantic.

[35] Across the Atlantic basin at 26.5°N, the model results yield a five-year mean AMOC transport of 18.2 Sv above ~1000 m, in a good agreement with 18.4 Sv based on the RAPID data. The vertical structure of the northward transport is also in good agreement. The modeled southward transports below 1000 m, however, are more concentrated in the upper NADW layer than observations. Although the issue of southward NADW being too shallow is somewhat similar to the results based on z-coordinate OGCMs, as discussed by *Saunders et al.* [2008], there is a key difference. The southward transport in HYCOM contains a

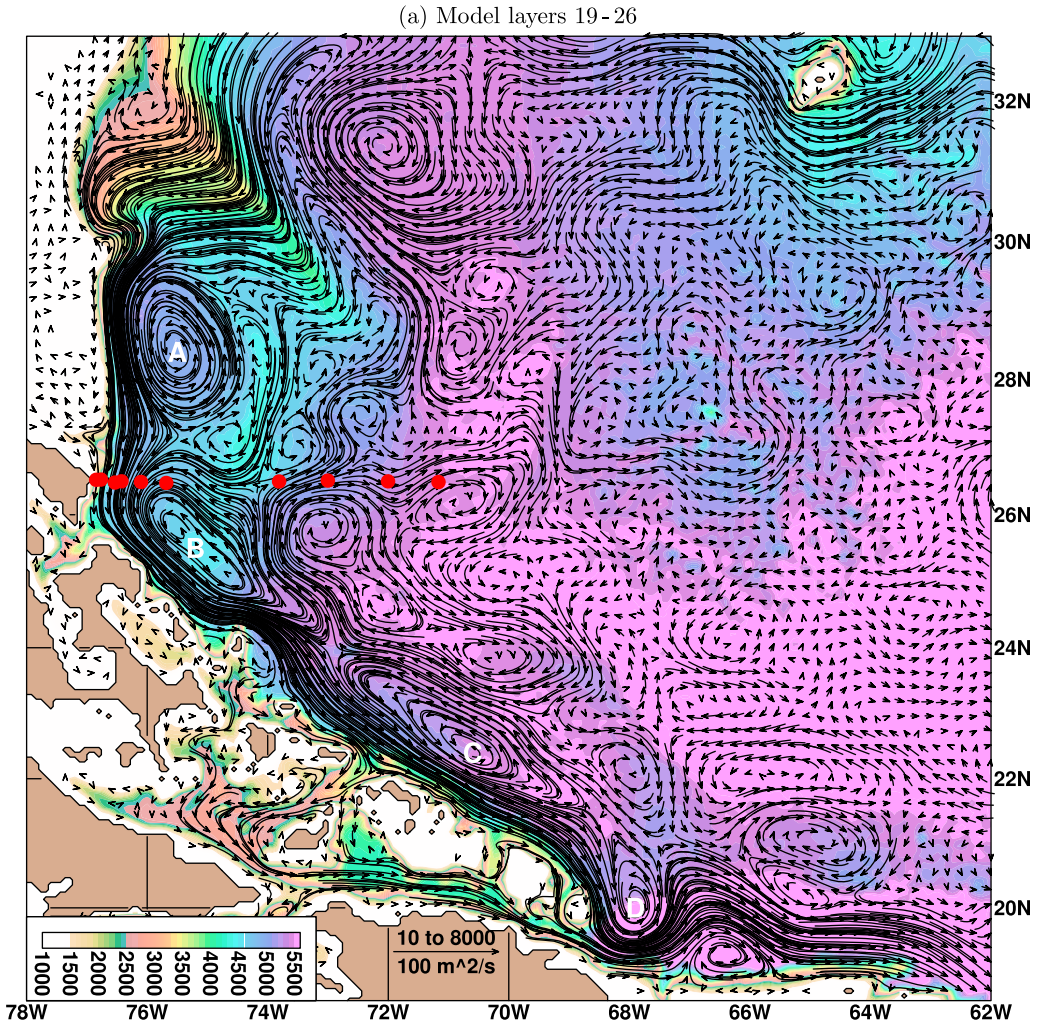

Figure 16. Modeled mean transport per unit width (in $m^2\ s^{-1}$) in the western subtropical North Atlantic from simulation E026 over years 16–20. (a) Model layers 19–26 (σ_2 of 36.52–37.02 kg m^{-3}), representing the upper North Atlantic deep water in a depth range of about 1000–3000 m. Labels A–D denote cyclonic gyres offshore of the DWBC. (b) Model layer 27 (σ_2 of 37.06 kg m^{-3}) to bottom, representing the lower North Atlantic deep water below about 3000 m. Labels A–C denote cyclonic gyres offshore of the DWBC.

secondary maximum near 4000 m corresponding to the NSOW contribution, not seen in the *z*-coordinate OGCMs.

[36] In the Florida Strait, the model-based FC has a mean transport of 30.8 Sv at 27°N, compared to the well-determined observed mean transport of 32.1 Sv [*Meinen et al.*, 2010]. The spatial distributions of the modeled velocity and water properties across the FC are also in close agreement with observations. Within a distance of 500 km east of Abaco along 26.5°N, the model results yield a net southward transport of 25.3 Sv below 1000 m. This net transport and the vertical structure are generally consistent with the data-based estimates [*Johns et al.*, 2008]. The model-based DWBC is narrower than observed [*Bryden et al.*, 2005b] and carries about 10% less in mean transport. The model indicates that this is due in part to flow above the Bahama Ridge, which is not resolved by the mooring arrays.

[37] The model-determined northward AMOC transport (18.2 Sv) contains a contribution of 4.1 Sv through the mid-ocean, primarily in the Ekman layer (3.2 Sv) but also below 600 m (0.9 Sv). The remaining 14.1 Sv flows through the Florida Strait. This modeled AMOC contribution accounts for about 45% of the total FC transport at 27°N and the results are consistent with an early estimate by *Schmitz and Richardson* [1991]. Breaking down the model transport into density layers, the northward limb of the AMOC consists of about 2/3 surface water and 1/3 upper AAIW. The thermocline water in between circulates horizontally within the subtropical gyre and does not contribute to the AMOC.

[38] The model results (Figure 16) depict a complicated deep circulation pattern in the western subtropical North Atlantic, as a result of bathymetric steering. Simply speaking, the flow in the layer of upper NADW primarily consists of a southward DWBC and northward recirculations along the eastern flank of the Bahama Ridge. In the layer of lower NADW, the northward recirculation is found farther offshore along the Hatteras Abyssal Plain. In addition to the DWBC, which flows eastward in the Puerto Rico Trench, a second branch of the DWBC flows eastward along the

(b) Model layer 27 to bottom

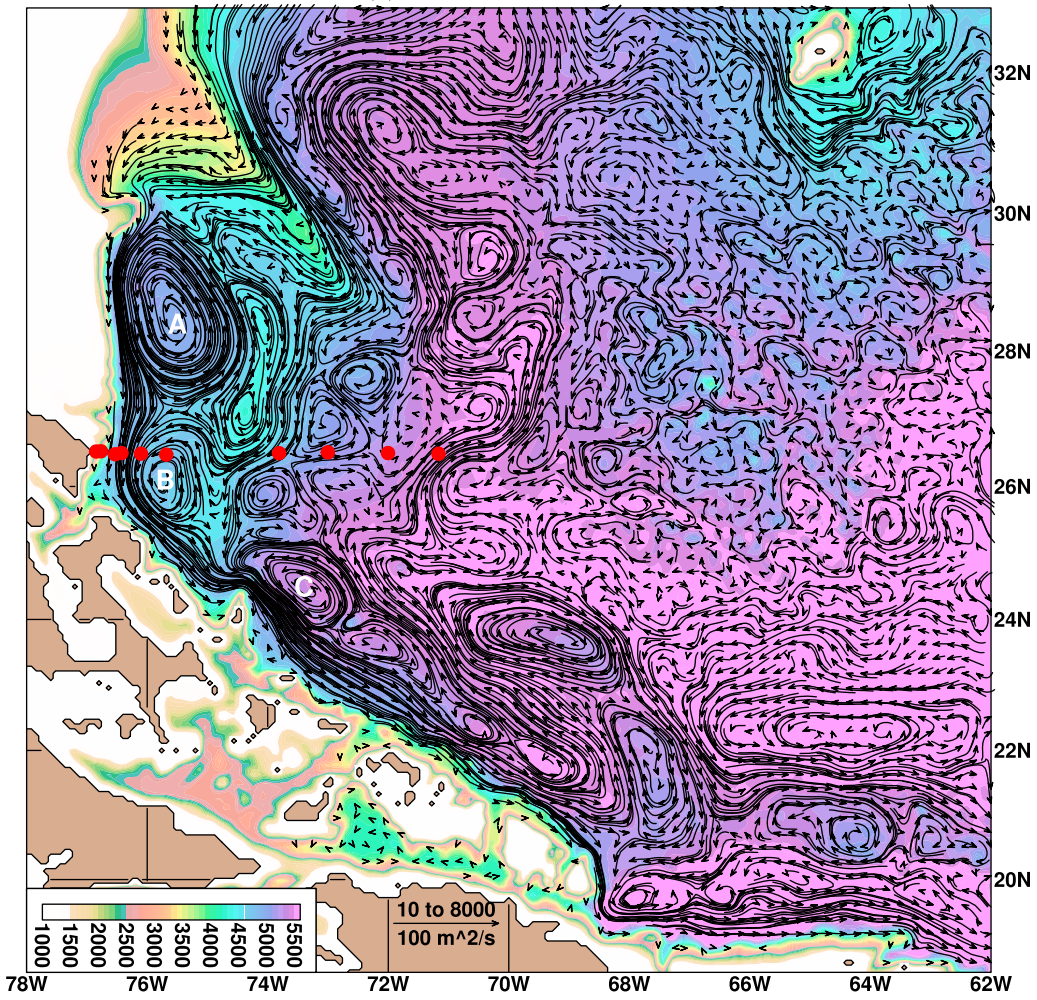

Figure 16. (continued)

northern flank of the Greater Antilles Outer Ridge. This circulation pattern is generally consistent with the results based on the moored array along 26.5°N [*Bryden et al.*, 2005b] and the flow pattern inferred by *Tucholke et al.* [1973].

[39] **Acknowledgments.** This work is a contribution to the project U. S.-GODAE: Global ocean prediction using the HYbrid Coordinate Ocean Model (HYCOM), funded under the National Ocean Partnership Program, and to the projects Global Remote Littoral Forcing via Deep Water Pathways (program element 601153N) and Full Column Mixing for Numerical Ocean Models (602435N), funded by the Office of Naval Research. The simulations were performed on supercomputers at the Naval Oceanographic Office, Stennis Space Center, Mississippi, using computer time provided by the U.S. Department of Defense High Performance Computing Modernization Program. Data from the RAPID-MOC monitoring project are freely available at http://www.noc.soton.ac.uk/rapidmoc, a project funded by the U.K. Natural Environment Research Council. H. Bryden and P. Saunders (NOC/UK), Y. Drillet (Mercator/FR), and R. Lumpkin (NOAA/AOML) kindly provided profiles from their papers. The authors thank A. J. Wallcraft and E. J. Metzger (NRL/SSC) for help in configuring the numerical experiments. The detailed comments of the two anonymous reviewers helped to improve the manuscript significantly. The authors have also been benefited from discussion with W. E. Johns (RSMAS/UM). This is Naval Research Laboratory publication number NRL/JA/7320–11-0805, and it has been approved for public release.

References

Amos, A., A. L. Gordon, and E. D. Schneider (1971), Water masses and circulation patterns in the region of the Blake-Bahama Outer Ridge, *Deep Sea Res., Part I*, *18*, 145–165.

Atkinson, L. P., T. Berger, P. Hamilton, E. Waddell, K. Leaman, and T. N. Lee (1995), Current meter observations in the Old Bahama Channel, *J. Geophys. Res.*, *100*(C5), 8555–8560, doi:10.1029/95JC00586.

Bleck, R. (2002), An oceanic general circulation model framed in hybrid isopycnic-Cartesian coordinates, *Ocean Modell.*, *37*, 55–88.

Bryden, H. L., H. R. Longworth, and S. A. Cunningham (2005a), Slowing of the Atlantic meridional overturning circulation at 25°N, *Nature*, *438*, 655–657.

Bryden, H. L., W. E. Johns, and P. M. Saunders (2005b), Deep western boundary current east of Abaco: Mean structure and transport, *J. Mar. Res.*, *63*, 35–57.

Carnes, M. R. (2009), Description and evaluation of GDEM-V3.0, *Tech. Rep. NRL/ MR/7330–09-9165*, 21 pp., Naval Res. Lab., Stennis Space Cent., Miss. [Available at http://www7320.nrlssc.navy.mil/pubs.php.]

Chassignet, E. P., L. T. Smith, G. R. Halliwell, and R. Bleck (2003), North Atlantic simulations with the hybrid coordinate ocean model (HYCOM): Impact of the vertical coordinate choice, reference pressure, and thermobaricity, *J. Phys. Oceanogr.*, *33*, 2504–2526.

Cunningham, S. A., et al. (2007), Temporal variability of the Atlantic meridional overturning circulation at 26.5°N, *Science*, *317*, 935–938.

Ganachaud, A., and C. Wunsch (2000), Improved estimates of global ocean circulation, heat transport and mixing from hydrographic data, *Nature*, *408*, 453–456.

Hall, M. M., and H. L. Bryden (1982), Direct estimates and mechanisms of ocean heat transport, *Deep Sea Res., Part I*, *29*(3A), 339–359.

Hall, M. M., T. M. Joyce, R. S. Pickart, W. M. Smethie, and D. J. Torres (2004), Zonal circulation across 52°W in the North Atlantic, *J. Geophys. Res.*, *109*, C11008, doi:10.1029/2003JC002103.

Hurlburt, H. E., and P. J. Hogan (2000), Impact of 1/8° to 1/64° resolution on Gulf Stream model-data comparisons in basin-scale subtropical Atlantic Ocean models, *Dyn. Atmos. Ocean*, *32*, 283–329.

Hurlburt, H. E., et al. (2011), Dynamical evaluation of ocean models using the Gulf Stream as an example, in *Operational Oceanography in the 21st Century*, edited by A. Schiller and G. B. Brassington, pp. 545–609, Springer, New York.

Hurrell, J. W. (1995), Decadal trends in the North Atlantic Oscillation: Regional temperatures and precipitation, *Science*, *269*(5224), 676–679.

Johns, E., R. A. Fine, and R. L. Molinari (1997), Deep flow along the western boundary south of the Blake Bahama Outer Ridge, *J. Phys. Oceanogr.*, *27*, 2187–2208.

Johns, W. E., T. L. Townsend, D. M. Fratantoni, and W. D. Wilson (2002), On the Atlantic inflow to the Caribbean Sea, *Deep Sea Res., Part I*, *49*(2), 211–243.

Johns, W. E., L. M. Beal, M. O. Baringer, J. R. Molina, S. A. Cunningham, T. Kanzow, and D. Rayner (2008), Variability of shallow and deep western boundary currents off the Bahamas during 2004–05: Results from the 26°N RAPID-MOC Array, *J. Phys. Oceanogr.*, *38*, 605–623.

Joyce, T. M., A. Hernandez-Guerra, and W. M. Smethie (2001), Zonal circulation in the NW Atlantic and Caribbean from a meridional World Ocean Circulation Experiment hydrographic section at 68°W, *J. Geophys. Res.*, *106*(C10), 22,095–22,113.

Kanzow, T., et al. (2007), Observed flow compensation associated with the MOC at 26.5°N in the Atlantic, *Science*, *317*, 938–941.

Kanzow, T., et al. (2010), Seasonal variability of the Atlantic meridional overturning circulation at 26.5°N, *J. Clim.*, *23*(21), 5678–5698, doi:10.1175/2010JCL13389.1.

Leaman, K. D., R. L. Molinari, and P. S. Vertes (1987), Structure and variability of the Florida Current at 27°N: April 1982–July 1984, *J. Phys. Oceanogr.*, *17*(5), 565–583.

Leaman, K. D., W. E. Johns, and T. Rossby (1989), The average distribution of volume transport and potential vorticity with temperature at three sections across the Gulf Stream, *J. Phys. Oceanogr.*, *19*, 36–51.

Leaman, K. D., P. S. Vertes, L. P. Atkinson, T. N. Lee, P. Hamilton, and E. Waddell (1995), Transport, potential vorticity, and current/temperature structure across Northwest Providence and Santaren Channels and the Florida Current off Cay Sal Bank, *J. Geophys. Res.*, *100*(C5), 8561–8569, doi:10.1029/94JC01436.

Lee, T. N., W. E. Johns, F. A. Schott, and R. J. Zantopp (1990), Western boundary current structure and variability east of Abaco, Bahamas at 26.5°N, *J. Phys. Oceanogr.*, *20*, 446–466.

Lee, T. N., W. E. Johns, R. J. Zantopp, and E. R. Fillenbaum (1996), Moored observations of western boundary current variability and thermohaline circulation at 26.5°N in the subtropical North Atlantic, *J. Phys. Oceanogr.*, *26*, 962–983.

Lumpkin, R., and K. G. Speer (2003), Large scale vertical and horizontal circulation in the North Atlantic Ocean, *J. Phys. Oceanogr.*, *33*, 1902–1920.

Meinen, C. S., M. O. Baringer, and R. F. Garcia (2010), Florida Current transport variability: An analysis of annual and longer-period signals, *Deep Sea Res., Part I*, *57*, 835–846.

Richardson, W. S., and J. R. Finlen (1967), The transport of Northwest Providence Channel, *Deep Sea Res., Part I*, *14*(3), 361–367.

Roemmich, D. (1980), Estimation of meridional heat flux in the North Atlantic by inverse methods, *J. Phys. Oceanogr.*, *10*, 1972–1983.

Roemmich, D., and C. Wunsch (1985), Two transatlantic sections: Meridional circulation and heat flux in the subtropical North Atlantic Ocean, *Deep Sea Res., Part I*, *32*(6), 619–664.

Rosmond, T., J. Teixeira, M. Peng, T. Hogan, and R. Pauley (2002), Navy Operational Global Atmospheric Prediction System (NOGAPS): Forcing for ocean models, *Oceanography*, *15*(1), 99–108.

Saunders, P. M., S. A. Cunningham, B. A. D. Cuevas, and A. C. Coward (2008), Comments on "Decadal changes in the North Atlantic and Pacific meridional overturning circulation and heat flux," *J. Phys. Oceanogr.*, *38*, 2104–2107.

Schmitz, W. J., Jr., and P. L. Richardson (1991), On the source of the Florida Current, *Deep Sea Res.*, *38*, S379–S409.

Smith, R. D., M. E. Maltrud, F. O. Bryan, and M. W. Hecht (2000), Numerical simulation of the North Atlantic Ocean at 1/10°, *J. Phys. Oceanogr.*, *30*, 1532–1561.

Tucholke, B. E., W. R. Wright, and C. D. Hollister (1973), Abyssal circulation over the Greater Antilles Outer Ridge, *Deep Sea Res., Part I*, *20*(11), 973–995.

Uppala, S. M., et al. (2005), The ERA-40 re-analysis, *Q. J. R. Meteorol. Soc.*, *131*, 2961–3012, doi:10.1256/qj.04.176.

Wunsch, C. (2005), The total meridional heat flux and its oceanic and atmospheric partition, *J. Clim.*, *18*, 4374–4380, doi:10.1175/JCLI3539.1.

Xu, X., W. J. Schmitz Jr., H. E. Hurlburt, P. J. Hogan, and E. P. Chassignet (2010), Transport of Nordic Seas overflow water into and within the Irminger Sea: An eddy-resolving simulation and observations, *J. Geophys. Res.*, *115*, C12048, doi:10.1029/2010JC006351.

P. J. Hogan and H. E. Hurlburt, Oceanography Division, Naval Research Laboratory, Stennis Space Center, MI 39529, USA.

W. J. Schmitz Jr., Harte Research Institute, Texas A&M University-Corpus Christi, 6914 Windy Creek Dr., Corpus Christi, TX 78414, USA.

X. Xu, Department of Marine Science, University of Southern Mississippi, 1020 Balch Blvd., Stennis Space Center, MS 39529, USA. (xiaobiao.xu@usm.edu)